Paper V

Feasibility of ultra-wideband SAW RFID tags meeting FCC rules

S. Härmä, V. P. Plessky, X. Li, and P. Hartogh

V

Feasibility of Ultra-Wideband SAW RFID Tags Meeting FCC Rules

Sanna Härmä, Victor P. Plessky, *Senior Member, IEEE*, Xianyi Li, and Paul Hartogh

***Abstract*— We discuss the feasibility of surface acoustic wave (SAW) radio-frequency identification (RFID) tags that rely on ultra-wideband (UWB) technology. We propose a design of a UWB SAW tag, carry out numerical experiments on the device performance, and study signal processing in the system. We also present experimental results for the proposed device and estimate the potentially achievable reading distance.**

UWB SAW tags will have an extremely small chip size ($<$ 0.5 x 1 mm^2) and a low cost. They also can provide a large number of different codes. The estimated read range for UWB SAW tags is about 2 m with a reader radiating as low as $<$ 0.1-mW power levels with an extremely low duty factor.

I. Introduction

THE currently emerging ultra-wideband (UWB) radio technology enables short-range communications with high speed and low power [1]. The use of wide-band (spread spectrum) and UWB signals in surface acoustic wave (SAW) sensors and SAW-device-based communication systems has been discussed by many authors [2]–[7]. However, the possibility of using UWB signals in SAW identification tags has not yet been addressed in detail in the literature, although the use of spread spectrum signals for tags has been discussed in a few publications [8]–[13]. Meanwhile, this possibility is especially attractive because, for SAW tags, the used frequency band B is of primary importance. The number of different codes that can be obtained is determined by the product BT [14], where T is the coding time duration. In SAW devices, T is normally limited to 2 μs to 4 μs because of high propagation loss at gigahertz frequencies. The availability of a rather wide ISM band (B = 82.5 MHz) at 2.45 GHz is the main argument for using this frequency band for "global SAW tags" [15], where in combination with a few microseconds of coding time, a 64-bit SAW tag has been demonstrated and 256-bit tags seem to be achievable.

However, using UWB signals allows for much wider bands and the same BT product can be achieved with significantly shorter delays. For example, at frequencies higher than 1.99 GHz, we can use, according to the FCC regulations [16], [17], signals with a fractional bandwidth greater than 20% and a power of -41.3 dBm/MHz (when SAW tags are treated as "surveillance systems"). Using a band of 500 MHz from 2.0 GHz to 2.5 GHz would satisfy the criterion on bandwidth. With B = 500 MHz, achieving a BT of 200 only requires a coding time of 400 ns instead of the 2 μs typical for 2.45-GHz SAW tags. Such a short delay corresponds to a propagation path length of only about 1.6 mm. The total length of a SAW tag that uses reflectors for encoding can thus be shorter than 1 mm. Moreover, with these frequencies, we remain in the area of standard SAW technology with optical lithography. SAW technology is thus perfectly mature for manufacturing such devices at low cost [4] and in big volumes.

Another attractive possibility related to the use of UWB technology is performing signal processing within a SAW tag. Using a chirp transducer in the tag allows for a matched-to-signal processing of the tag response. In this case, the dispersion of the interrogation signal is modified within the tag. The tag response thus differs from the reflections of the interrogation signal from other objects. This makes the system more resistant to echoes from the surroundings. Typically, an initial delay of 1 μs is needed in ordinary SAW tags for the decay of environmental echoes. With UWB tags, this delay can be significantly shorter.

A shorter total delay also implies lower propagation losses. A propagation time of 400 ns corresponds to only about -3 dB of propagation loss. In ordinary SAW tags, the total delay is about 2 μs to 4 μs, and propagation loss correspondingly on the order of -20 dB. UWB SAW tags may then have a reduced total loss despite the increased loss in the dispersive transducer.

Finally, the reader power may be very low for UWB tags. In the below example, the total power radiated by a reader is lower than 40 μW. This is undeniably an attractive level, although the reading range is expected to be limited to about 2 m to 5 m depending on integration time and other reader characteristics. For short reading distances, the interrogation signal will be radiated for about 1 ms per one reading. This puts the average power at the nanowatt level, assuming reading of one tag per second sufficient for many applications.

In what follows, we will propose a design of a UWB SAW tag, carry out numerical experiments on the device performance using the Matlab software and a FEM-BEM simulator, and study signal processing in the system. We will also present experimental results for the proposed device and compare those with a simulated response. Finally, we will estimate the potentially achievable reading distance.

II. Proposed UWB SAW Tag and Numerical Experiments

We propose a SAW tag consisting of a chirp transducer, for processing linear frequency modulated (LFM) signals, and a series of wide-band code reflectors, as depicted schematically

S. Härmä and V. P. Plessky are with the Department of Applied Physics, Helsinki University of Technology, P. O. Box 3500, FI-02015 TKK, Finland. V. P. Plessky is also with GVR Trade SA, Bevaix, Switzerland. X. Li and P. Hartogh are with the Max Planck Institute for Solar System Research, Katlenburg-Lindau, Germany.

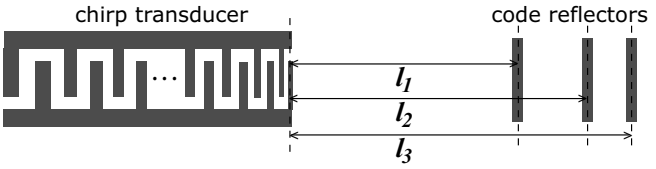

Fig. 1. A schematic drawing of a SAW tag consisting of a chirp transducer and an array of wide-band code reflectors.

in Fig. 1. The code reflectors include only one or a few narrow open-circuit electrodes each [18].

As discussed above, the initial delay (corresponding to the round-trip propagation of SAWs between the transducer and the first code reflector) can be drastically reduced from 1 μs, typically used for ordinary SAW tags. In our examples, we use an initial delay of either 50 ns (in Section II-A) or 150 ns (in II-B). These correspond to respective distances l_1 of 100 μm and 300 μm (on 128°-$LiNbO_3$) from the transducer to the first code reflector.

We have chosen to use a band of B = 500 MHz and, hence, the shortest possible pulse is about 2 ns wide. This is also the minimum time slot for positioning the code reflectors. One time slot of 2 ns roughly corresponds to a 4-μm slot on the substrate surface. With a coding time of 400 ns, we have 200 time slots. Using time position encoding [19] with 5 slots per group [18], we can have up to 40 reflectors, which corresponds to at least 64 bits available for coding. Such a device will be about 1 mm long and 0.5 mm wide. With single-metal-layer photolithography, this chip will not be expensive.

Below, we will first illustrate the principles of signal processing within the proposed SAW tag using ideal LFM signals. We will then take a more practical approach and study SAW tag performance by carrying out numerical experiments using a FEM-BEM simulator. The studied devices operate at a center frequency of f_c = 1 GHz but the same principles can be transferred to the 2-GHz range. A relatively low frequency was chosen in order to keep the running time of the FEM-BEM simulation (reported in Section II-B) reasonable. For higher frequencies, a significantly larger number of transducer electrodes is needed to produce a chirp of certain duration. The simulation time increases quickly with the increase of the number of electrodes.

A. Simulation with Ideal Signals

We first illustrate the operating principle of the proposed SAW tag by using ideal theoretical signals. The length of the chirp transducer on the tag corresponds to a SAW propagation delay of $T_{\rm chirp}$, and the pitch of transducer electrodes changes gradually such that the instantaneous frequency corresponding to the electrode structure is linearly dependent on time. In this example, $T_{\rm chirp}$ = 100 ns and B = 500 MHz ($BT_{\rm chirp}$ = 50). With f_c = 1 GHz, this corresponds to a transducer with 100 pairs of electrodes and a length of about 400 μm.

For "interrogation", we use Matlab software to simulate up- and down-chirps with the parameters B and $T_{\rm chirp}$ specified

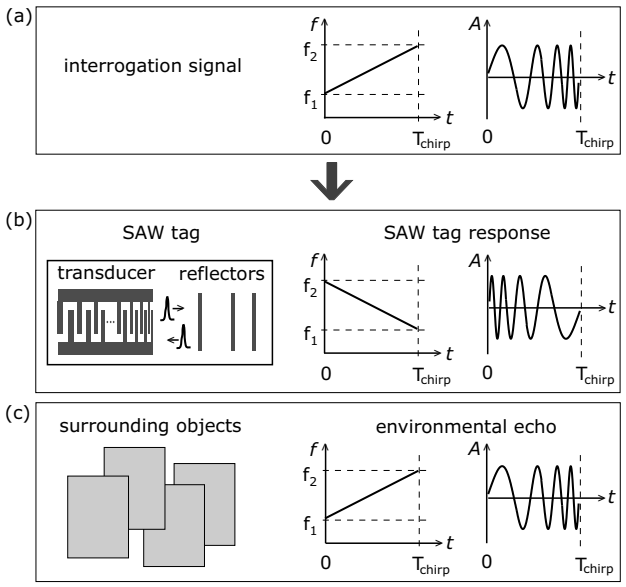

Fig. 2. Interrogation process. (a) An up-chirp LFM signal is used for interrogation. (b) The signal is compressed by the chirp transducer, reflected by the code reflectors, and expanded by the transducer. The output has a dispersion opposite to that of the interrogation signal. (c) Reflections from surrounding objects have the same dispersion as the interrogation signal.

above. These signals can be written as:

$$A_{\rm up}(t) = e^{j\left(\pi\mu\left(t-\frac{T_{\rm chirp}}{2}\right)^2+2\pi f_c\left(t-\frac{T_{\rm chirp}}{2}\right)\right)} \quad (1)$$

$$A_{\rm down}(t) = e^{j\left(-\pi\mu\left(t-\frac{T_{\rm chirp}}{2}\right)^2+2\pi f_c\left(t-\frac{T_{\rm chirp}}{2}\right)\right)} \quad (2)$$

for $0 \le t \le T_{\rm chirp}$. In (1) and (2), the chirp rate μ is defined as $\mu = B/T_{\rm chirp}$.

For simulating one of the possibilities of "reading" the tag, we imagine, that the chirp transducer on the SAW tag is excited with a chirp pulse having a dispersion opposite to that of the transducer (to create a situation where the transducer is matched to the signal). For the tag depicted in Fig. 1, an up-chirp would be used for interrogation (see Figs 2a and 2b). In this way, the signal propagating on the surface of the substrate will be a compressed pulse of width $1/B$ = 2 ns. In order to improve the sidelobe level of the compressed pulse, we weight the interrogation signal using a cosine window. The above tag is thus actually excited by a pulse of form

$$A_{\rm up,w}(t) = A_{\rm up}(t)\cos\left(\frac{\pi t}{T_{\rm chirp}} - \frac{\pi}{2}\right). \quad (3)$$

The spectrum of the compressed pulse can be presented as a product of the spectrum of the interrogation pulse $A_{\rm up,w}(f)$ and the frequency response $A_{\rm down}(f)$ of the chirped transducer

$$A_{\rm compr}(f) = A_{\rm up,w}(f)A_{\rm down}(f)L. \quad (4)$$

A loss factor L is included here to account for transduction, mismatch, propagation, and other losses.

The compressed pulse is then partially reflected by code reflectors. In this example, the tag has three reflectors, placed at round-trip time delays of t_1 = 50 ns, t_2 = 100 ns, and

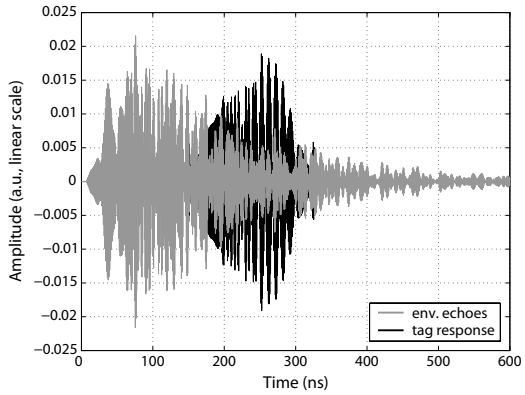

Fig. 3. Real parts of the tag output and the environmental echoes. Matlab simulation.

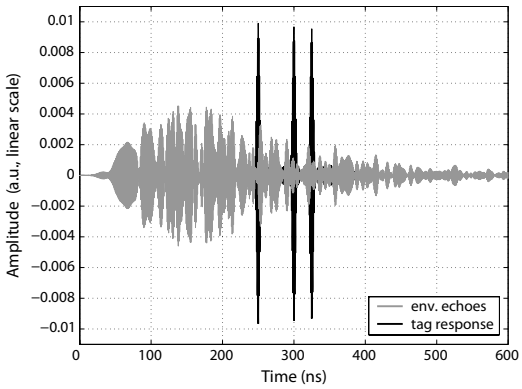

Fig. 4. Real parts of the tag response and the environmental echoes after being processed with a dispersive delay line matched to the tag response. Matlab simulation.

t_3 = 125 ns from the transducer. These time delays roughly correspond to distances of l_1 = 100 μm, l_2 = 200 μm, and l_3 = 250 μm (on 128°-$LiNbO_3$). We describe the contribution of the reflectors as

$$R(f) = R_0 \sum_{i=1}^{3} e^{j \cdot 2\pi f \cdot t_i}, \tag{5}$$

where a reflectivity of R_0 = 10% is assumed for each reflector. The reflected pulse train will be received by the chirp transducer, which in our example will first output high frequencies and then low frequencies. The spectrum of the output signal will have the form

$$A_{\mathrm{out}}(f) = A_{\mathrm{compr}}(f) R(f) A_{\mathrm{down}}(f). \tag{6}$$

In the time domain, this is an expanded pulse with a dispersion opposite to the original interrogation signal (see Fig. 2b), according to which it is recompressed at the reader.

The environmental echoes, that is, the reflections of the interrogation signal from surrounding objects (outside the tag), are modeled by summing many reflected pulses with random amplitudes R_i and random delays τ_i as follows:

$$E(f) = \sum_{i=1}^{N} R_i e^{j \cdot 2\pi f \cdot \tau_i}. \tag{7}$$

In this equation, the amplitudes are supposed to decay with increasing delay. The total level of environmental echoes is adjusted to the level of the above described tag response, which determines the number N of included environmental echoes. In this example, N = 200.

The chirp pulse reflected by surrounding objects has a spectrum of

$$A_{\mathrm{env}}(f) = A_{\mathrm{up,w}}(f) E(f). \tag{8}$$

As illustrated in Fig. 2c, the environmental echoes have the same dispersion as the original interrogation signal, and hence opposite to the dispersion of the tag response. As a result, while the tag response is compressed at the reader, the environmental echoes are not.

The simulated tag response $A_{\mathrm{out}}(t)$ and the environmental echoes $A_{\mathrm{env}}(t)$ are shown in Fig. 3. For clarity, the two signals are separated in time in this example, but they could as well coincide. The studied tag device has three reflectors and the response contains three overlapping chirp signals. The environmental echoes are supposed to be comparable in amplitude with the tag response, but after being processed with a dispersive delay line matched to the tag response, the amplitude of the tag response is clearly increased above that of the environmental echoes, as can be seen in Fig. 4.

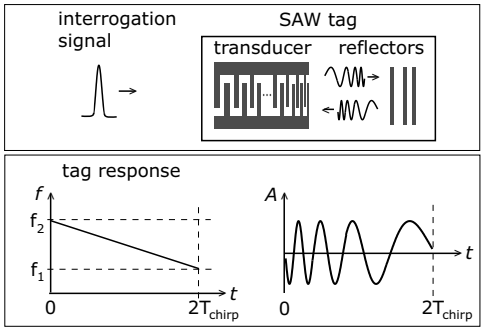

Fig. 5. Interrogation of SAW tag with a delta pulse.

Another possibility to read the tag is to use a short delta pulse as an interrogation signal (see Fig. 5). In this case, the signal propagating on the chip surface is an expanded pulse having the same dispersion as the transducer. When signals reflected from the code reflectors are received by the transducer, the beginning of the reflected signal is output first, while the end must travel through the entire transducer before being output. The duration of the tag response will then correspond to twice the time length of the transducer. The response is compressed using an LFM signal with a band of B = 500 MHz and a duration of $2T_{\mathrm{chirp}}$ = 200 ns. One more possibility to read the tag would be to use an up-chirp interrogation signal with a band of B and a duration of $2T_{\mathrm{chirp}}$. This would result in short compressed pulses being reflected back by the tag. These examples illustrate that there are many ways of reading a tag having a chirp transducer. All these methods profit from the fact that the tag response is different from the interrogation signal and its parameters are known in advance so that a matched-to-signal reading is possible.

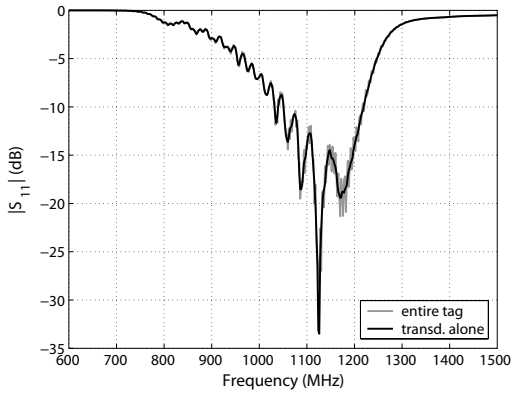

Fig. 6. $|S_{11}|$ in the frequency domain for the entire single-reflector SAW tag device and for the chirp transducer alone. FEM-BEM simulation.

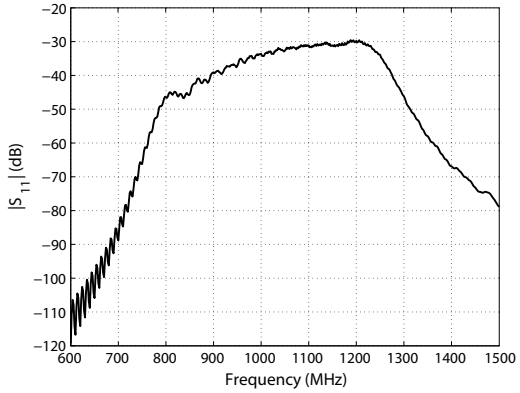

Fig. 7. $|S_{11}|$ in the frequency domain for the single-reflector SAW tag device after subtraction of the signal directly reflected from the chirp transducer. FEM-BEM simulation.

B. Numerical Experiments Using a FEM-BEM Simulator

We numerically simulated the performance of a SAW tag similar to that sketched in Fig. 1. The simulated device consists of a chirp transducer and a single open-circuit electrode acting as a code reflector. The dispersion of the transducer is as illustrated in Fig. 1. It has the high frequency sections closest to the code reflector, that is, it is a down-chirp device that first generates high frequencies and then low frequencies. The transducer has the same parameters as in the previous example: B = 500 MHz, $T_{\rm chirp}$ = 100 ns, μ = 5 MHz/ns, and f_c = 1 GHz. It has N_p = 100 pairs of electrodes and a length of about 400 μm. The distance between the transducer and the code reflector is l_1 = 300 μm, which roughly corresponds to a round-trip time delay of 150 ns on 128°-$LiNbO_3$. The metal thickness relative to wavelength is 3%, and the metal ratio for the transducer structure is 0.5. The code reflector has a width of 1.2 μm.

1) Results of FEM-BEM Simulation: We simulated the structure with FEMSAW, a FEM-BEM-based [20] simulation software that produces the S_{11} parameters of the device. The simulation was separately run for the entire single-reflector tag described above and for its chirp transducer alone. Fig. 6 shows the absolute value of S_{11} for both of these cases. The results of the latter simulation were used to eliminate the contribution of the direct reflection of the electromagnetic (EM) signal from the transducer. The S_{11} of the transducer was subtracted from the S_{11} of the entire single-reflector tag. The subtraction was performed in linear scale for the real and imaginary parts of S_{11}. Here we profit from the advantages of numerical experiments: the transducers are perfectly identical in the two simulations, which would not necessarily be the case in a real experiment with two separate packaged devices. Fig. 7 presents the result of the subtraction.

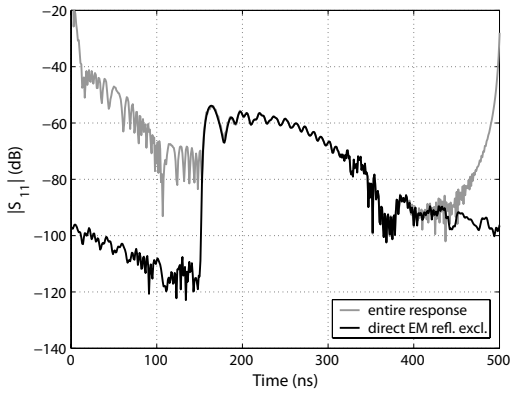

Fig. 8. $|S_{11}|$ in the time domain for the entire single-reflector SAW tag device and for the case where the direct EM reflection from the transducer has been excluded. FEM-BEM simulation.

Fig. 8 shows the impulse response of the tag for two cases: first, $|S_{11}|$ for the entire tag and, second, for the case where the direct EM reflection has been eliminated. As expected, the reception of the signal reflected from the code reflector starts at 150 ns and ends at 350 ns. The chirp duration is doubled compared to the propagation time inside the chirp transducer since this inverse-Fourier-transformed signal corresponds to the case where the initial interrogation signal is a delta pulse. As can be seen from Figs. 6 to 8, we have not tried to optimize the device performance. The objective of this paper is merely to prove a concept.

The tag response of Fig. 8 could now be compressed using a cosine-weighted up-chirp with a duration $2T_{\rm chirp}$ (see e.g. Fig. 5). However, we use here theoretical LFM signals for interrogation in order to illustrate signal processing in different steps.

2) Chirp Interrogation of Simulated Device: We "interrogate" the simulated tag device with the up-chirp signal introduced in (3). The tag response is shown in Fig. 9. The interrogation pulse is 100 ns long, and the signal observed between 0 ns and 100 ns thus is the direct reflection of the interrogation pulse from the tag's transducer. The transducer length also corresponds to a delay of 100 ns, that is, a compressed pulse is completely formed (and regenerated) at the delay of 100 ns, where a sharp peak can be observed. The distance between the transducer and the reflector corresponds to a round-trip delay of 150 ns. Hence, the reflection of the compressed pulse from the code reflector is output between 250 ns and 350 ns. High frequencies are output first and low frequencies last.

Although the origin of the peak at 250 ns still demands

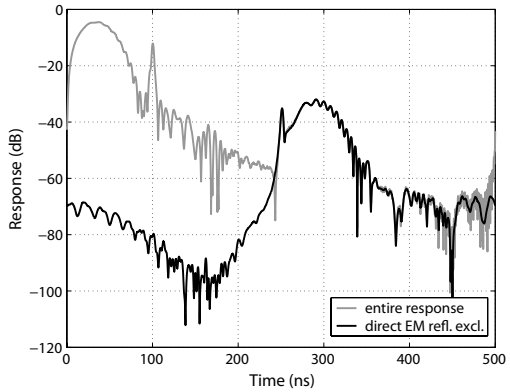

Fig. 9. Tag response to an up-chirp signal for the entire single-reflector SAW tag device and for the case where the direct EM reflection from the transducer has been excluded. FEM-BEM simulation.

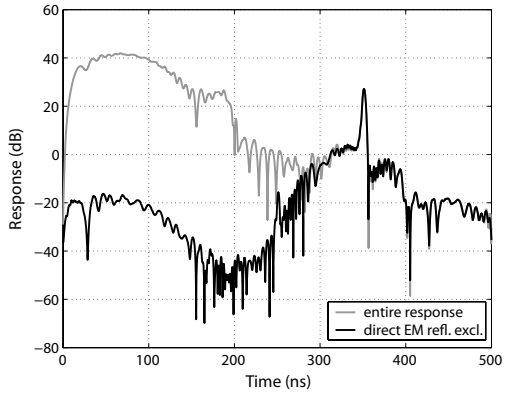

Fig. 10. Tag responses of Fig. 9 after compression by an ideal up-chirp correlator.

investigations, further simulations give reason to assume that the peak is caused by an end effect of the transducer edge. Inside the transducer, the effective region [21] is surrounded by regions that receive the pulse out of phase. The edge of the transducer, however, has such a region on one side only. The number of electrode pairs N_{eff} in the effective region can be obtained from

$$N_{\text{eff}}(f) = \frac{f}{f_c\sqrt{BT_{\text{chirp}}}} N_p. \tag{9}$$

For example, at the center of our chirp transducer, there are about 14 effective electrode pairs. The end effects were reduced when the simulated transducer was prolonged by adding $N_{\text{eff}}/2$ electrode pairs to both ends of the transducer. The added electrodes were alternately connected to the two busbars and had a gradually decreasing width. This gave a correspondingly decreasing coupling into surface acoustic waves.

The tag response of Fig. 9 is compressed using a theoretically simulated ideal up-chirp correlator (Eq. 1). Fig. 10 shows the result of compression. The direct reflection from the transducer (from 0 ns to 100 ns in Fig. 9) now has the same dispersion as the correlator and no compressed peak is observed. Also the wide-band peak observed at 100 ns in Fig. 9 has been expanded. However, the code reflection has a dispersion opposite to that of the correlator and a compressed code pulse is detected. The compressed pulse is about 25 dB above the noise level.

Fig. 11. Fabricated SAW tag device. Structure length is 1.1 mm.

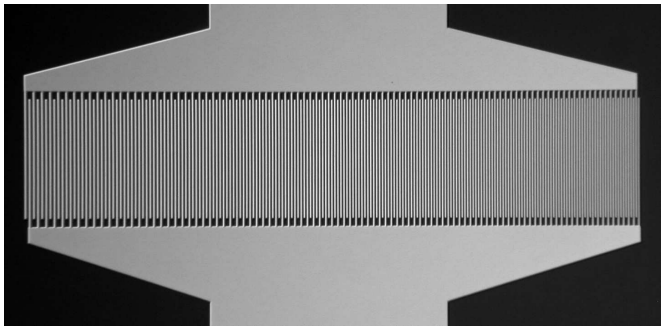

Fig. 12. Chirp transducer of fabricated SAW tag device. Aperture is 75 μm and length is 400 μm. Critical dimension is 0.77 μm. Center frequency is 1 GHz.

III. Experimental results

We also designed a SAW tag device having the same transducer as the above described tags but 10 code reflectors. Encoding was based on groups of 5 slots, as described above, with a slot width of 5 ns and an initial delay of 150 ns. The device was simulated using FEMSAW and fabricated on 128°-$LiNbO_3$ using electron beam lithography and liftoff process. The fabricated device is shown in Fig. 11 and its chirp transducer in Fig. 12.

The experimental tag device is "interrogated" using the procedure described in context with Figs 9 and 10. The tag response to the up-chirp signal of (3) is shown in Fig. 13. The immediate compressed pulse is observed at 100 ns. The response signal contains 10 overlapping chirped code reflections between about 250 ns and 550 ns.

Figs 14 and 15 show the compressed responses in the simulated and experimental cases, respectively. These responses are obtained by applying an ideal chirp correlator with band B = 500 MHz and chirp duration $2T_{\text{chirp}}$ = 200 ns directly to the simulated or measured S_{11} data. The level of compressed peaks is comparable between the two cases. The compressed peaks are 15 dB to 20 dB above the noise level, but the reflector strengths have not been optimized in this case. Some energy evidently passes through the entire device. Both responses illustrate the fact that the total delay is significantly shorter than with ordinary SAW tags.

IV. Reading Range Estimation

In this section, we roughly estimate the achievable reading distance for a UWB SAW tag that operates within the 2.0-GHz

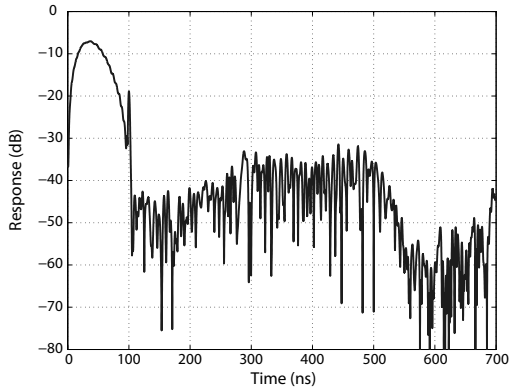

Fig. 13. Tag response to an up-chirp interrogation signal. The response contains 10 overlapping chirped code reflections between 250 ns and 550 ns. Experimental data.

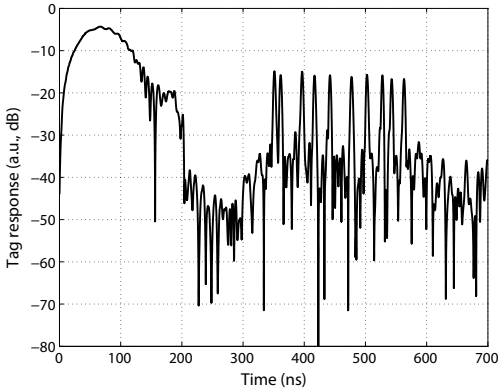

Fig. 14. Compressed response of a SAW tag device having 10 code reflectors. Simulated data.

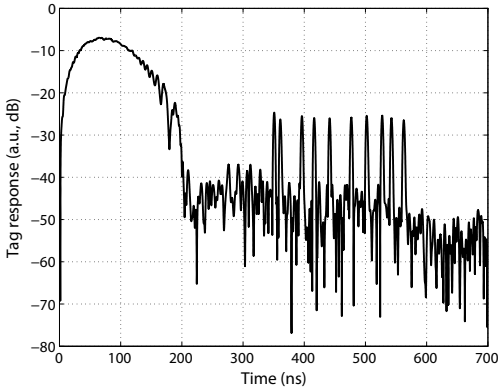

Fig. 15. Compressed response of a SAW tag device having 10 code reflectors. Experimental data.

to 2.5-GHz frequency range and satisfies the FCC rules.

The reading range r is determined by the radar equation [22], [23]:

$$r = \frac{\lambda}{4\pi} \sqrt[4]{\frac{P_{\mathrm{t,reader}} G_{\mathrm{reader}}^2 G_{\mathrm{tag}}^2 T_i}{L_{\mathrm{tot}} \cdot kT_0 F \cdot SNR}}, \qquad (10)$$

where λ is the electromagnetic wavelength (0.13 m at 2.25 GHz), $P_{\mathrm{t,reader}}$ is the power transmitted by the reader, G_{reader} and G_{tag} are the respective gains of the reader and tag antennas, and T_i is the signal integration time, accounting for the accumulation of signal due to multiple readings. L_{tot} is the total loss in the system including SAW propagation losses and losses in the tag but excluding losses due to propagation and spreading of EM waves. k is the Boltzmann constant, T_0 is the absolute temperature, and F is the noise figure deteriorating the sensitivity of the receiver. SNR is the signal-to-noise ratio required for the desired probability of the correct deciphering of the code [24], [25]. A high SNR guarantees a high probability of correct reading of the code, but reduces the reading distance, as can be seen from (10).

The radiated power is limited by the FCC rules for ultra-wideband applications. The three important points are [16], [17]:

- The equivalent isotropically radiated power (EIRP), that is, the product of the power supplied to the antenna $P_{\mathrm{t,reader}}$ and the antenna gain G_{reader} in a given direction, is limited to -41.3 dBm/MHz at frequencies higher than 1.99 GHz for "surveillance systems".
- At this frequency range, emissions are to be measured using a resolution bandwidth of 1 MHz.
- Within a 50-MHz bandwidth centered on f_M (the frequency corresponding to the maximal spectral density of the signal power), peak emissions are limited to 0 dBm EIRP (or, if a resolution bandwidth RBW other than 50 MHz is used, to $20 \cdot \log(RBW/50)$ dBm, where RBW is in MHz).

In a 500-MHz band (2.0 GHz to 2.5 GHz), the continuously radiated power $P_{\mathrm{t,reader}} G_{\mathrm{reader}}$ must not exceed $10^{-4.13} \cdot 500$ mW = 37 μW. However, the reader might have a low duty factor and be silent for most of the time. How can the above cited rules then be interpreted? The emission measurement method is also determined in the FCC rules [16]. For power level measurements of signals with frequency higher than 960 MHz, a "1 millisecond or less averaging time" is specified. That means that the first point above basically limits the total energy radiated during 1 ms to 37 μW $\cdot$ 1 ms = 37 nJ. Actually only this total radiated energy $P_{\mathrm{t,reader}} G_{\mathrm{reader}} T_i$ enters the equation (10) and determines the reading range. Substituting this energy into (10), we obtain a reading distance of 2.4 m. Fig. 16 shows the reading range r as a function of the integration time T_i. In these estimations, we have used the following values: G_{reader} = 10 dBi, G_{tag} = 0 dBi, T_0 = 300 K, and F = 5 dB. L_{tot} is estimated as 40 dB and SNR is taken as 1.

If the radiated signals have a shorter duration than 1 ms, the peak power can be higher. According to the third point above, the peak power can reach 0.1 W in a 500-MHz band but then the total duration of emission must be about 0.37 μs within a repetition time of at least 1 ms. Using such relatively high power pulses may be a better option for a reader, especially if accumulation of readings during many milliseconds is acceptable. Although key issues in a UWB SAW tag system, the reader and antenna technologies fall outside the scope of this paper.

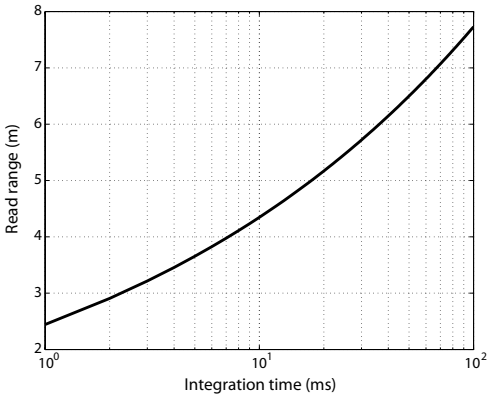

Fig. 16. Estimated read range r as a function of reader integration time T_i for a 2.25-GHz UWB SAW tag satisfying the FCC rules.

V. Discussion and Conclusions

Recently, a UWB SAW correlator operating within the FCC [16] designated band for developmental UWB communication devices was demonstrated [6], and we believe that also SAW RFID tags ideally match with UWB technology. In this paper, we have shown through simulations, experiments, and estimations that UWB SAW tags meeting the FCC rules are feasible. We have presented experimental evidence, that UWB SAW tags can have a reasonably large data capacity of one million different codes in a chip length of about 1 mm. Our estimations also show that UWB SAW tags can be interrogated with low-power readers and a reading range of a few meters can be achieved, depending on the integration time and other reader characteristics.

UWB SAW tags combine a small chip size with a reasonably large data capacity. In addition, the on-tag signal processing permitted by LFM signals and a chirp transducer allows for a strong resistance to environmental interference. UWB SAW tags also have much shorter delays than standard SAW tags. This will result in significantly lower propagation losses. These great advantages should overcome numerous difficulties related to design, loss level, temperature sensitivity, etc. that we are prepared to meet in the ongoing experimental realization of UWB SAW tags. The unusual substrate materials, such as 41°-$LiNbO_3$, having excellent coupling but some additional "leaky" loss mechanisms, can be considered valid candidates for substrates [26] for UWB devices. UWB technology opens an attractive perspective of development of extremely small, cheap, and completely passive tags operating with readers radiating only microwatts of power.

Acknowledgements

S. Härmä acknowledges the financial support granted by the Nokia Foundation and the Finnish Concordia Fund. The authors thank Clinton S. Hartmann for fruitful discussions, especially concerning the reading range estimations.

References

[1] D. Porcino and W. Hirt, "Ultra-wideband radio technology: potential and challenges ahead", *IEEE Communications Magazine*, vol. 41, no. 7, pp. 66-74, July 2003.

[2] A. Pohl, G. Ostermayer, L. Reindl, and F Seifert, "Spread spectrum techniques for wirelessly interrogable passive SAW sensors", in *Proc. IEEE 4th International Symposium on Spread Spectrum Techniques and Applications*, vol. 2, Sept. 1996, pp. 730-734.

[3] A. Springer, M. Huemer, L. Reindl, C. Ruppel, A. Pohl, F. Seifert, W. Gugler, and R. Weigel, "A robust ultra-broad-band wireless communication system using SAW chirped delay lines", *IEEE Trans. Microwave Theory Tech.*, vol. 46, no. 12, pp. 2213-2219, Dec. 1998.

[4] M. Chomiki, "SAW-based solutions for UWB communication", *2005 European Microwave Conference*, vol. 3, Oct. 2005.

[5] Nanotron Technologies, "nanoNET Chirp Based Wireless Networks", http://www.nanotron.com/EN/docs/WP/WP_CSS.pdf.

[6] R. Brocato, J. Skinner, G. Wouters, J. Wendt, E. Heller, and J. Blaich, "Ultra-wideband SAW correlator", *IEEE Trans. Ultrason., Ferroelectr., Freq. Contr.*, vol. 53, no. 9, pp. 1554-1556, Sept. 2006.

[7] D. Gallagher, D. Malocha, D. Puccio, and N. Saldanha, "Orthogonal frequency coded filters for use in ultra-wideband communication systems", *IEEE Trans. Ultrason., Ferroelectr., Freq. Contr.*, vol. 55, no. 3, pp. 696-703, March 2008.

[8] E. Mariani, "Passive SAW-ID tags using a chirp transducer", U. S. Patent no. 5469170, 1995.

[9] T. Yoshihiko, "SAW-ID-tag device using chirp signal", Patent no. JP11145874, 1999.

[10] Z. Ianelli and M. Koslar, "Surface-wave transducer device and identification system with such device", U. S. Patent no. 6788204, 2004.

[11] A. Stelzer, M. Pichler, S. Scheiblhofer, and S. Schuster, "Identification of SAW ID-tags using an FSCW interrogation unit and model-based evaluation", *IEEE Trans. Ultrason., Ferroelectr., Freq. Contr.*, vol. 51, no. 11, pp. 1412-1420, Nov. 2004.

[12] D. Puccio, D. C. Malocha, N. Saldanha, D. R. Gallagher, and J. H. Hines, "Orthogonal frequency coding for SAW tagging and sensors", *IEEE Trans. Ultrason., Ferroelectr., Freq. Contr.*, vol. 53, no. 2, pp. 377-384, Feb. 2006.

[13] D. C. Malocha, J. Pavlina, D. Gallagher, N. Kozlovski, B. Fisher, N. Saldanha, and D. Puccio, "Orthogonal frequency coded SAW sensors and RFID design principles", in *Proc. IEEE International Frequency Control Symposium*, May 2008, pp. 278-283.

[14] C. E. Shannon, "A mathematical theory of communication", in *The Bell System Technical Journal*, vol. 27, pp. 379-423, 623-656, July, Oct. 1948.

[15] C. Hartmann, P. Brown, and J. Bellamy, "Design of global SAW RFID tag devices", in *Proc. 2nd Int. Symp. Acoustic Wave Devices for Future Mobile Commun. Syst.*, March 2004, pp. 15-19.

[16] "Technical requirements applicable to all UWB devices", Code of Federal Regulations, Title 47, Chapter I, Part 15, §15.521.

[17] G. Breed, "A summary of FCC rules for ultra wideband communications", *High Frequency Electronics*, vol. 4, no.1, pp. 42-44, Jan. 2005.

[18] S. Härmä, W. Arthur, C. Hartmann, R. Maev, and V. Plessky, "Inline SAW RFID tag using time position and phase encoding", in *Proc. IEEE Ultrason. Symp.*, 2007, pp. 1239-1242.

[19] R. Stierlin and R. Küng, "Process for carrying out a non-contact remote enquiry", U. S. Patent no. 6407695, 2002.

[20] P. Ventura, J. Hodé, M. Solal, J. Desbois, and J. Ribbe, "Numerical methods for SAW propagation characterization", in *Proc. IEEE Ultrason. Symp.*, 1998, pp. 175-186.

[21] D. Morgan, *Surface-Wave Devices for Signal Processing*. Amsterdam: Elsevier, 1991.

[22] L. Reindl, A. Pohl, G. Scholl, and R. Weigel, "SAW-based radio sensor systems", *IEEE Sensors Journal*, vol. 1, no. 1, pp. 69-78, June 2001.

[23] L. Blake, "Prediction of radar range", in M. Skolnik, *Radar Handbook*. Boston, MA: McGraw-Hill, 1990.

[24] S. Schuster, S. Scheiblhofer, L. Reindl, and A. Stelzer, "Performance evaluation of algorithms for SAW-based temperature measurement", *IEEE Trans. Ultrason., Ferroelectr., Freq. Contr.*, vol. 53, no. 6, pp. 1177-1185, June 2006.

[25] J. H. Kuypers, L. M. Reindl, S. Tanaka, and M. Esashi, "Maximum accuracy evaluation scheme for wireless SAW delay-line sensors", *IEEE Trans. Ultrason., Ferroelectr., Freq. Contr.*, vol. 55, no. 7, pp. 1640-1652, July 2008.

[26] K. Lee, W. Wang, T. Kim and S. Yang, "A novel 440 MHz wireless SAW microsensor integrated with pressure-temperature sensors and ID tag", *J. Micromech. Microeng.*, vol. 17, pp. 515-523, 2007.

Sanna Härmä was born in Kotka, Finland, in 1977. She received the Master of Science and Licentiate of Science (in Technology) degrees from the Helsinki University of Technology (TKK), Espoo, Finland, in 2001 and 2007, and the Bachelor of Arts degree (in French philology) from the University of Helsinki, Helsinki, Finland, in 2007.

She has worked as a research assistant at the Laboratory of Biomedical Engineering, TKK, as a research scientist at the Materials Physics Laboratory, TKK, as a design engineer at Thales Microsonics, Sophia-Antipolis, France, and as a subject teacher in Helsinki, Finland. She is currently preparing a D.Sc. thesis on SAW RFID tags at the Department of Applied Physics, TKK.

Victor P. Plessky was born in Belarus in 1952. He received the Ph.D. degree from the Moscow Physical-Technical Institute in 1978 and the D.Sc. degree from the Institute of Radio Engineering and Electronics (IRE, Russian Academy of Sciences, Moscow) in 1987. He was awarded the USSR National Award for Young Scientists in 1984.

He started to work at IRE in 1978 as a junior researcher and was promoted to laboratory director in 1987. In 1991, he also worked as a part-time professor at the Patris Lumumba University, Moscow. He received the full professor title in 1995 from the Russian Government.

In 1992, he joined Ascom Microsystems SA, Bevaix, Switzerland, where he worked as a SAW project manager. Since 1997, he has lectured on various SAW topics at the Helsinki University of Technology (TKK), Espoo, Finland, as a visiting professor and currently holds a docentship at TKK. In 1998, he started to work at the Neuchâtel office (Switzerland) of Thomson Microsonics (later Thales Microsonics, finally Temex), and since 2002 he has worked as a consultant.

Dr. Plessky has been engaged in research on semiconductor physics, SAW physics (new types of waves, scattering and reflection on surface irregularities, and laser generation of SAW), SAW device development (filters, delay lines, and reflective array compressors), and magnetostatic wave studies. His current interests focus on SAW physics and low-loss SAW filter development.

Xianyi Li was born in Xinjiang Province, China, in 1981. He received his Master degree in Electronic Engineering from the University of Electronic Science and Technology of China, Chengdu, Sichuan, China, in 2006. He is currently a Ph.D. student in the Max Planck Institute for Solar System Research, Katlenburg-Lindau, Germany. He works on the development of large bandwidth chirp transform spectrometers in the Chirp Transform Spectrometer team of the Planet Group.

Paul Hartogh was born in Germany in 1959. He received his PhD degree from the University of Goettingen in 1989. Since 1990, he has been a staff member with the Max Planck Institute for Solar System Research (MPS), Katlenburg-Lindau, Germany. He pioneered the development of chirp transform spectrometers for microwave remote sensing applications and is co-investigator of numerous space projects applying microwave heterodyne spectroscopy in the millimeter- and submillimeter-wave range, e.g., the Microwave Atmospheric Sounder (MAS) on the ATLAS 1-3 missions, the Microwave Instrument for the Rosetta Orbiter (MIRO), the Heterodyne Instrument for the Far Infrared (HIFI) on the Herschel Space Observatory, and the German Receiver for Astronomy at Terahertz frequencies (GREAT) on the Stratospheric Observatory for Infrared Astronomy. He has authored or coauthored approximately 120 papers. He is an editor of Atmospheric Chemistry and Physics and Advances in Geosciences. He is interested in chemistry and physics of atmospheres in the solar system (planets, moons, and comets) with some focus on the terrestrial planets and works on modeling and analysis/interpretation of atmospheric data derived from microwave measurements. He continues the development of high-performance chirp transform spectrometers for space applications aiming at integrated low-power designs with multigigahertz bandwidth. Dr. Hartogh is member of the International Commission on Planetary Atmospheres and their Evolution (ICPAE) and the ALOMAR Scientific Advisory Committee.